Available online at www.sciencedirect.com
SCIENCE DIRECT®
ELSEVIER
International Journal of Solids and Structures 43 (2006) 3875–3894
INTERNATIONAL JOURNAL OF SOLIDS and STRUCTURES
www.elsevier.com/locate/ijsolstr

A reciprocity theorem in linear gradient elasticity and the corresponding Saint-Venant principle

A.E. Giannakopoulos [a,*], E. Amanatidou [b], N. Aravas [b]

[a] Department of Civil Engineering, University of Thessaly, Volos 38336, Greece
[b] Department of Mechanical and Industrial Engineering, University of Thessaly, Volos 38336, Greece

Received 27 August 2004; received in revised form 22 April 2005

Abstract

In many practical applications of nanotechnology and in microelectromechanical devices, typical structural components are in the form of beams, plates, shells and membranes. When the scale of such components is very small, the material microstructural lengths become important and strain gradient elasticity can provide useful material modelling. In addition, small scale beams and bars can be used as test specimens for measuring the lengths that enter the constitutive equations of gradient elasticity. It is then useful to be able to apply approximate solutions for the extension, shear and flexure of slender bodies. Such approach requires the existence of some form of the Saint-Venant principle. The present work presents a statement of the Saint-Venant principle in the context of linear strain gradient elasticity. A reciprocity theorem analogous to Betti's theorem in classic elasticity is provided first, together with necessary restrictions on the constitutive equations and the body forces. It is shown that the order of magnitude of displacements are in accord with the Sternberg's statement of the Saint-Venant principle. The cases of stretching, shearing and bending of a beam were examined in detail, using two-dimensional finite elements. The numerical examples confirmed the theoretical results.

Keywords: Reciprocity theorem; Castigliano's theorems; Saint-Venant's principle; Strain gradient elasticity; Finite element models; Microelectromechanical devices

1. Introduction

Nanocomposites as well as macro-composites such as concrete and fiber-reinforced composites are typical materials that at very small volumes can be modelled by strain gradient type of constitutive equations.

* Corresponding author. Fax: +30 421 074 169.
E-mail address: civileng@civ.uth.gr (A.E. Giannakopoulos).

0020-7683/$ - see front matter © 2005 Elsevier Ltd. All rights reserved.
doi:10.1016/j.ijsolstr.2005.05.048

In many practical applications of nanotechnology and in microelectromechanical devices, typical structural components are in the form of beams, plates, shells and membranes (e.g. actuators and sensors). In such cases, material microstructural lengths become important and strain gradient elasticity can provide useful material modelling. Two major obstacles to a wider application of strain gradient elasticity are the lack of information about the material constants that are used in the constitutive equations and the complexity of the general theories involved. Regarding the first obstacle, static experiments can be designed based on slender structural configurations (e.g. cantilever and three-point bending tests). Regarding the second obstacle, engineering type of theories that account for strain gradient effects (e.g. Papargyri-Beskou et al., 2003, Tsepoura et al., 2002) have appeared and require the assurance of the Saint-Venant principle regarding loading and dimensions.

A detailed formulation and the general proof of Saint-Venant's principle in the context of linear elasticity were given by Sternberg (1954). Based on this general approach, Naghdi (1960) presented the Saint-Venant principle in the context of the linear theory of thin elastic shells and plates. A thorough review of methodologies and results related to Saint-Venant's principle can be found in the work of Horgan and Knowles (1983). The Saint-Venant principle was extended by Berglund (1977) to micropolar solids and was investigated numerically (in two-dimensions) by Nakamura and Lakes (1995). The general extension of the Saint-Venant principle in the context of the linear strain gradient elasticity (which includes as a special case the micropolar elasticity) seems to be lacking. Yet, the principle is tacitly assumed in a plethora of cases where microbeams, microplates and micromembranes model microelectromechanical systems (MEMS).

In classical elasticity, the proof of the Saint-Venant principle follows from Betti's reciprocal theorem, Sternberg (1954). Obviously, a general form of the reciprocal theorem has to be stated for the liner strain-gradient elasticity as well. In this context, we have to mention the work of Polyzos et al. (2003) who proved a reciprocal identity for a specific constitutive form of an isotropic, linear elastic solid with microstructure. As Boley (1958) pointed out, the linear ellipticity of the problem may imply integral representation of the displacements through the fundamental solution of the controlling linear differential equations and therefore the validity of Saint-Venant principle. The explicit fundamental solution for the displacements of a general isotropic linear elastic strain-gradient solid can be found in the work of Mindlin (1964).

The paper is structured as follows. First, the reciprocity theorem is stated in a general form, within the general constitutive framework of Mindlin's theory, Mindlin (1964). Particular forms for isotropy are also discussed. The Saint-Venant principle is established by appropriate Taylor expansion of the surface tractions and double stresses around fixed points on the surface. As side results of the reciprocity theorem, the Castigliano theorems are also derived. The exponential decay of the energy density along a slender beam with equilibrated loads at one end is estimated. Using the finite element method, we performed numerical investigations of stretching, shearing and bending of a beam, modelled as a two dimensional plane strain solid. The paper concludes with the assessment of the approximate strain-gradient beam theories.

2. Reciprocity theorem for linear strain-gradient elasticity

The theoretical proofs that follow are based on the Type II formulation of strain gradient elasticity, established by Mindlin (1964). We will use Cartesian coordinates, $x_i (i = 1, 2, 3)$, with the usual summation of repeated Latin indices from 1 to 3 and of repeated Greek indices from 1 to 2. The starting point is the virtual work statement. We assume a kinematically admissible field of virtual displacements, u_i^*, that obeys prescribed boundary conditions on part of the surface S of an elastic body of volume V:

$$u_i^* = u_i^0 \tag{1}$$

and

$$\frac{\partial u_i^*}{\partial n} \equiv u_{i,j}^* \quad n_j = \frac{\partial u_i^0}{\partial n} \tag{2}$$

Note that n_i is the unit normal vector to the surface that points outside the body and the comma denotes partial differentiation with respect to the coordinate indicated by the index that follows. The small strain tensor, ϵ_{ij}^*, corresponds to the kinematically admissible displacement field and is given by

$$\epsilon_{ij}^* = (u_{i,j}^* + u_{j,i}^*)/2 \tag{3}$$

The Cauchy stresses, τ_{ij}, and the double stresses, μ_{ijk}, obey the equilibrium equations, which in the presence of body forces F_i and body double forces Φ_{ji}, are

$$(\tau_{ji} - \mu_{kji,k} - \Phi_{ji})_{,j} + F_i = 0 \tag{4}$$

The assumption of a strain energy density $W(\epsilon_{ij}, \epsilon_{kl,m})$ imply:

$$\tau_{ij} = \tau_{ji} = \frac{\partial W}{\partial \epsilon_{ij}}, \quad \mu_{ijk} = \mu_{ikj} = \frac{\partial W}{\partial \epsilon_{jk,i}} \tag{5}$$

The surface tractions, P_i, are related to τ_{ij} and μ_{ijk} through the relations

$$P_i = n_j(\tau_{ji} - \mu_{kji,k} - \Phi_{ji}) - [D_j - (D_p n_p)n_j](n_k \mu_{kji}) \tag{6}$$

where D_i is the surface gradient operator

$$D_i = \frac{\partial}{\partial x_i} - n_k n_i \frac{\partial}{\partial x_k} \tag{7}$$

The double stresses produce boundary conditions of the type

$$R_i = n_k n_j \mu_{jki} \tag{8}$$

In case of non-smooth boundaries along lines C_a with tangent unit vector s_i, the surface jump stresses across these lines are

$$E_i = \| l_j n_k \mu_{kji} \| \tag{9}$$

where $l_i = e_{ijk} s_j n_k$ (e_{ijk} is the Levi–Civita permutation symbol). For smooth surfaces, $E_i = 0$. For plane problems, the lines C_a are actually corner points.

In case when $\Phi_{ji} \neq 0$, we cannot establish a general reciprocal form and we will further assume that $\Phi_{ji} = 0$.

The Cauchy and double stresses satisfy prescribed dynamic boundary conditions

$$P_i = P_i^0 \tag{10}$$

$$R_i = R_i^0 \tag{11}$$

$$E_i = E_i^0 \tag{12}$$

For each direction x_i, the above dynamic conditions apply on the surface S of the body so that: for the part of S where condition (10) holds, condition (1) does not apply and for the part of S where condition (11) holds, condition (2) does not apply.

The virtual work statement is

$$\int_V (\tau_{ij}\epsilon_{ij}^* + \mu_{ijk}\epsilon_{jk,i}^*)\,\mathrm{d}V = \int_V F_i u_i^*\,\mathrm{d}V + \int_S \left(P_i u_i^* + R_i \frac{\partial u_i^*}{\partial n}\right)\mathrm{d}S + \sum_a \oint_{C_a} E_i u_i^*\,\mathrm{d}S \tag{13}$$

Assuming a linear elastic energy potential, Mindlin (1964), the general forms of the constitutive equations are

$$\tau_{pq} = c_{pqij}\epsilon_{ij} + f_{ijkpq}\epsilon_{jk,i} \tag{14}$$

$$\mu_{pqr} = a_{pqrijk}\epsilon_{jk,i} + f_{pqrij}\epsilon_{ij} \tag{15}$$

In the above forms, the elastic constants $c_{ijkl} = c_{klij}$ have the usual symmetries of the pairs (i,j) and (k,l), with dimension $[N/m^2]$. The elastic constants $a_{lmnijk} = a_{ijklmn}$ have additional symmetries of the pairs (j,k) and (m,n), with dimension $[N]$. The additional material constants $f_{ijklm} = f_{ikjlm}$ have additional symmetries of the pair (l,m), with dimension $[N/m]$. Obviously, microstructural lengths can be incorporated in a_{lmnijk} and surface energies in f_{ijklm}. It can be shown that a reciprocal theorem can be stated only if $f_{ijklm} = 0$ (which is always true for isotropic solids) and we will further assume it is so.

Due to the symmetries of the remaining constants $(c_{pqij}; a_{pqrijk})$, it can be shown that

$$\tau_{ij}\epsilon^*_{ij} = \tau^*_{ij}\epsilon_{ij}, \quad \mu_{ijk}\epsilon^*_{jk,i} = \mu^*_{ijk}\epsilon_{jk,i} \tag{16}$$

where

$$\tau^*_{ij} = c_{ijkl}\epsilon^*_{kl}, \quad \mu^*_{lmn} = a_{lmnijk}\epsilon^*_{jk,i} \tag{17}$$

From τ^*_{ij} and μ^*_{ijk}, we can define P^*_i, R^*_i, E^*_i and F^*_i, using Eqs. (6), (8), (9) and (4), respectively (i.e., the statically admissible generalized tractions). Then, Eq. (13) can be casted in the form

$$\int_V (\tau^*_{ij}\epsilon_{ij} + \mu^*_{ijk}\epsilon_{jk,i})\,\mathrm{d}V = \int_V F^*_i u_i\,\mathrm{d}V + \int_S \left(P^*_i u_i + R^*_i \frac{\partial u_i}{\partial n}\right)\mathrm{d}S + \sum_a \oint_{C_a} E^*_i u_i\,\mathrm{d}s \tag{18}$$

where u_i are the displacements that corresponds to ϵ_{ij} (rigid body displacements are excluded).

Combining Eqs. (13), (18) and (16), we obtain the following reciprocity form:

$$\begin{aligned}&\int_V F_i u^*_i\,\mathrm{d}V + \int_S \left(P_i u^*_i + R_i \frac{\partial u^*_i}{\partial n}\right)\mathrm{d}S + \sum_a \oint_{C_a} E_i u^*_i\,\mathrm{d}S \\ &\quad = \int_V F^*_i u_i\,\mathrm{d}V + \int_S \left(P^*_i u_i + R^*_i \frac{\partial u_i}{\partial n}\right)\mathrm{d}S + \sum_a \oint_{C_a} E^*_i u_i\,\mathrm{d}s\end{aligned} \tag{19}$$

We emphasize again the importance of the requirement $f_{ijklm} = 0$, a natural fact for the isotropic response (see Appendix A for a summary of isotropic constitutive equations). Assuming a priori $f_{ijklm} = 0$ and $\Phi_{ji} = 0$, Eq. (19) can be proven directly, using the divergence theorem.[1]

For smooth boundaries, Eq. (19) simplifies to

$$\int_V F_i u^*_i\,\mathrm{d}V + \int_S \left(P_i u^*_i + R_i \frac{\partial u^*_i}{\partial n}\right)\mathrm{d}S = \int_V F^*_i u_i\,\mathrm{d}V + \int_S \left(P^*_i u_i + R^*_i \frac{\partial u_i}{\partial n}\right)\mathrm{d}S \tag{20a}$$

and in the absence of body forces

$$\int_S \left(P_i u^*_i + R_i \frac{\partial u^*_i}{\partial n}\right)\mathrm{d}S = \int_S \left(P^*_i u_i + R^*_i \frac{\partial u_i}{\partial n}\right)\mathrm{d}S \tag{20b}$$

Eqs. (19) and (20) agree with the particular results of Polyzos et al. (2003). In the case of classic elasticity, $\mu_{ijk} = 0$ and Eq. (20b) becomes the familiar Betti's reciprocal form (Love, 1927),

$$\int_V F_i u^*_i\,\mathrm{d}V + \int_S (n_i\tau_{ji})u^*_i\,\mathrm{d}S = \int_V F^*_i u_i\,\mathrm{d}V + \int_S (n_i\tau^*_{ji})u_i\,\mathrm{d}S \tag{21}$$

[1] The authors are grateful to one of the reviewers that brought this to our attention.

3. Castigliano's theorems

A side result of the reciprocity theorem is the Castigliano identities, of particular use in statically indeterminate structures. Starting from Eq. (13), we assume that $F_i = 0$ and $E_i = 0$ and take as virtual displacements the differentials of the actual displacements, that is $u_i^* = \mathrm{d}u_i$. Then, Eq. (13) becomes

$$\int_V (\tau_{ij}\mathrm{d}\epsilon_{ij} + \mu_{ijk}\mathrm{d}\epsilon_{jk,i})\,\mathrm{d}V = \int_S \left[P_i\,\mathrm{d}u_i + R_i\,\mathrm{d}\left(\frac{\partial u_i}{\partial n}\right)\right]\mathrm{d}S \tag{22}$$

Remembering that the analysis is in the context of small deformations, the first term of Eq. (22) is actually the total differential of the elastic energy U and so

$$\mathrm{d}U \equiv \int_V \mathrm{d}W\,\mathrm{d}V = \int_S \left[P_i\,\mathrm{d}u_i + R_i\,\mathrm{d}\left(\frac{\partial u_i}{\partial n}\right)\right]\mathrm{d}S \tag{23}$$

We consider now the case where a number of concentrated generalized forces and double forces are applied on the surface of the body, i.e.,

$$\mathbf{P}(\mathbf{x}) = \sum_{n=1}^{N} P^{(n)}\mathbf{p}^{(n)}\delta(\mathbf{x}-\mathbf{x}^{(n)}) \quad \text{and} \quad \mathbf{R}(\mathbf{x}) = \sum_{m=1}^{M} R^{(m)}\mathbf{r}^{(m)}\delta(\mathbf{x}-\mathbf{x}^{(m)}) \tag{24}$$

where M and N is the number concentrated generalized forces and double forces, respectively, $\delta(\mathbf{x})$ is the Dirac-delta function, $\mathbf{p}^{(n)}$ and $\mathbf{r}^{(m)}$ are unit vectors that define the direction of the forces, $P^{(n)}$ and $R^{(m)}$ are the corresponding magnitudes, and $\mathbf{x}^{(n)}$ and $\mathbf{x}^{(m)}$ are the corresponding points of application. When these loads are used in (23), the result is

$$\mathrm{d}U = \sum_{n=1}^{N} P^{(n)}\,\mathrm{d}u^{(n)} + \sum_{m=1}^{M} R^{(m)}\,\mathrm{d}\left(\frac{\partial u^{(m)}}{\partial n}\right) \tag{25a}$$

where $u^{(n)} = \mathbf{u}(\mathbf{x}^{(n)})\cdot\mathbf{p}^{(n)}$ and $u^{(m)} = \mathbf{u}(\mathbf{x}^{(m)})\cdot\mathbf{r}^{(m)}$, i.e., $u^{(n)}$ and $u^{(m)}$ are the components of the displacements in the direction of the applied loads at their points of application.

If we consider the elastic energy as a function of the displacements and their normal derivatives at the points of application of the concentrated loads,

$$U = U\left(u^{(1)},\ldots,u^{(N)};\quad \frac{\partial u^{(1)}}{\partial n},\ldots,\frac{\partial u^{(M)}}{\partial n}\right) \tag{25b}$$

then we conclude from (24b) that

$$P^{(n)} = \frac{\partial U}{\partial u^{(n)}} \quad \text{and} \quad R^{(m)} = \frac{\partial U}{\partial(\partial u^{(m)}/\partial n)} \tag{25c}$$

which are the forms of Castigliano's first theorem.

Provided we can invert uniquely Eqs. (14) and (15) and express $\epsilon_{ij} = \epsilon_{ij}(\tau_{kl})$, $\epsilon_{mn,q} = \epsilon_{mn,q}(\mu_{prs})$, the complementary strain energy density is

$$W^c(\tau_{ij},\mu_{klm}) = \frac{1}{2}(\tau_{ij}\epsilon_{ij} + \mu_{klm}\epsilon_{kl,m}) \tag{26}$$

Assume $F_i = 0$ and $E_i = 0$ and take $\tau_{ij}^* = \mathrm{d}\tau_{ij}$ and $\mu_{ijk}^* = \mathrm{d}\mu_{ijk}$, that is the differentials of the actual Cauchy stresses and double stresses. Then Eq. (18) becomes

$$\int_V (\mathrm{d}\tau_{ij}\epsilon_{ij} + \mathrm{d}\mu_{ijk}\epsilon_{jk,i})\,\mathrm{d}V = \int_S \left(\mathrm{d}P_i u_i + \mathrm{d}R_i\frac{\partial u_i}{\partial n}\right)\mathrm{d}S \tag{27}$$

The first term of Eq. (27) is the total differential of the complementary elastic energy and so

$$\mathrm{d}U^c \equiv \int_V \mathrm{d}W^c\,\mathrm{d}V = \int_S \left(u_i\,\mathrm{d}P_i + \frac{\partial u_i}{\partial n}\,\mathrm{d}R_i\right)\mathrm{d}S \tag{28a}$$

Following similar arguments to those which led to Eq. (25b) and assuming now that $U^c = U^c(P^{(1)},\ldots,P^{(N)};R^{(1)},\ldots,R^{(M)})$, we conclude that

$$u^{(n)} = \frac{\partial U^c}{\partial P^{(n)}} \quad \text{and} \quad \frac{\partial u^{(m)}}{\partial n} = \frac{\partial U^c}{\partial R^{(m)}} \tag{28b}$$

which are the forms of Castigliano's second theorem.

4. The Saint-Venant principle for linear strain-gradient elastic bodies

4.1. Integral representation for surface displacements and their normal derivatives

Focusing on bodies with smooth boundaries and ignoring body forces, we can specify P_i^* and R_i^* in such a way so that the reciprocity relation yields general expressions for the values of displacements and their normal derivatives on the surface of the elastic body.

At a point $\mathbf{x}^0$ on the surface, we can select local orthogonal coordinates (ξ_1,ξ_2) that span a region of small radius ϵ around $\mathbf{x}^0$ (subsurface S_ϵ). Assume

$$P_i^{*(k)} = \frac{\delta_{ki}}{\pi\epsilon^2} \text{ only on } S_\epsilon \quad \text{and} \quad R_i^* = 0 \text{ on } S \tag{29}$$

where δ_{k_i} is the delta of Kronecker. In the limit $\epsilon \to 0$,

$$\int_S \left(P_i^{*(k)}u_i + R_i^*\frac{\partial u_i}{\partial n}\right)\mathrm{d}S = \int_{S_\epsilon} \frac{u_k}{\pi\epsilon^2}\,\mathrm{d}S \to u_k(\mathbf{x}^0) \tag{30}$$

Similarly we can select

$$R_i^{*(l)} = \frac{\delta_{l_i}}{\pi\epsilon^2} \text{ only on } S_\epsilon \quad \text{and} \quad P_i^* = 0 \text{ on } S \tag{31}$$

In the limit $\epsilon \to 0$,

$$\int_S \left(P_i^*u_i + R_i^{*(l)}\frac{\partial u_i}{\partial n}\right)\mathrm{d}S = \int_{S_\epsilon} \frac{\partial u_l}{\partial n}\frac{1}{\pi\epsilon^2}\,\mathrm{d}S \to \frac{\partial u_l}{\partial n}(\mathbf{x}^0) \tag{32}$$

With the above selections of P_i^* and R_i^*, the reciprocal form (20b) gives

$$u_k(\mathbf{x}^0) = \int_S \left(P_i u_i^{*(k)} + R_i\frac{\partial u_i^{*(k)}}{\partial n}\right)\mathrm{d}S \tag{33}$$

for the selection of (29), and

$$\frac{\partial u_l}{\partial n}(\mathbf{x}^0) = \int_S \left(P_i u_i^{*(l)} + R_i\frac{\partial u_i^{*(l)}}{\partial n}\right)\mathrm{d}S \tag{34}$$

for the selection of (31). Note that in Eq. (33), the displacements $u_i^{*(k)}$ are the results of the applied loads given by (29). In Eq. (34), the displacements $u_i^{*(l)}$ are the results of the applied loads given by (31). The linearity of the constitutive equations permits superposition in cases we have both $P_i^{*(k)}$ and $R_i^{*(l)}$.

It should be noted that the above results can be obtained alternatively, by specifying the unit point loads as $P_i^{*(k)}(\mathbf{x}) = \delta_{ki}\delta(\mathbf{x}-\mathbf{x}^0)$ and $R_i^{*(l)}(\mathbf{x}) = \delta_{li}\delta(\mathbf{x}-\mathbf{x}^0)$.

4.2. Sternberg's statement of the Saint-Venant principle

Consider the Taylor expansion of the displacements u_i about the surface point $\mathbf{x}^0$, with respect to the surface orthogonal coordinates (ξ_1,ξ_2) defined in the previous section. Then, from Eq. (33) we have

$$u_k(\mathbf{x}^0) = u_i^{*(k)}(\mathbf{x}^0)\int_S P_i\,\mathrm{d}S + \frac{\partial u_i^{*(k)}}{\partial n}(\mathbf{x}^0)\int_S R_i\,\mathrm{d}S + \frac{\partial u_i^{*(k)}}{\partial \xi_\alpha}(\mathbf{x}^0)\int_S P_i\xi_\alpha\,\mathrm{d}S + \frac{\partial}{\partial \xi_\alpha}\frac{\partial u_i^{*(k)}}{\partial n}(\mathbf{x}^0)\int_S R_i\xi_\alpha\,\mathrm{d}S + \text{Higer Order Terms} \tag{35}$$

Similarly, we can formulate the corresponding Taylor expansion of the normal derivative of the displacements $\partial u_i/\partial n$, using Eq. (34). The conditions for the existence of the above expansions are implied.

If P_i and R_i are bounded, then we have the following cases regarding the order of magnitude of u_i and $\partial u_i/\partial n$, as $\epsilon \to 0$:

(a) If $\int_S P_i\,\mathrm{d}S \neq 0$ and/or $\int_S R_i\,\mathrm{d}S \neq 0$, then

$$u_i^{*(k)}(\mathbf{x}^0) = \mathrm{O}(\epsilon^2) \quad \text{and} \quad \frac{\partial u_i^{*(k)}}{\partial \xi_\alpha}(\mathbf{x}^0) = \mathrm{O}(\epsilon^2) \text{ or smaller} \tag{36}$$

(b) If $\int_S P_i\,\mathrm{d}S = \int_S R_i\,\mathrm{d}S = 0$, then

$$u_i^{*(k)}(\mathbf{x}^0) = \mathrm{O}(\epsilon^3) \quad \text{and} \quad \frac{\partial u_i^{*(k)}}{\partial \xi_\alpha}(\mathbf{x}^0) = \mathrm{O}(\epsilon^3) \text{ or smaller} \tag{37}$$

This case corresponds to no resultant load.

(c) If $\int_S P_i\,\mathrm{d}S = \int_S R_i\,\mathrm{d}S = \int_S P_i\xi_\alpha\,\mathrm{d}S = \int_S R_i\xi_\alpha\,\mathrm{d}S = 0$, then

$$u_i^{*(k)}(\mathbf{x}^0) = \mathrm{O}(\epsilon^4) \quad \text{and} \quad \frac{\partial u_i^{*(k)}}{\partial \xi_\alpha}(\mathbf{x}^0) = \mathrm{O}(\epsilon^4) \text{ or smaller} \tag{38}$$

This case corresponds to self equilibrated load.

(d) Astatic equilibrium is defined when the applied generalized tractions (P_i and R_i) are parallel and remain in self equilibrium under an arbitrary change of the coordinate system. In such case:

$$u_i^{*(k)}(\mathbf{x}^0) = \mathrm{O}(\epsilon^4) \quad \text{and} \quad \frac{\partial u_i^{*(k)}}{\partial \xi_\alpha}(\mathbf{x}^0) = \mathrm{O}(\epsilon^4) \tag{39}$$

The above results can be extended to the case of applied concentrated forces and moments, double forces and double moments (i.e $P_i^{(k)}(\mathbf{x}) = \delta_{ki}\delta(\mathbf{x}-\mathbf{x}^0)$ and $R_i^{(l)}(\mathbf{x}) = \delta_{li}\delta(\mathbf{x}-\mathbf{x}^0)$). Then, the orders of magnitude found above $[\mathrm{O}(\epsilon^2),\mathrm{O}(\epsilon^3),\mathrm{O}(\epsilon^4)]$ are replaced with $[\mathrm{O}(1),\mathrm{O}(\epsilon),\mathrm{O}(\epsilon^2)]$, respectively. Note that these results are in accord with Sternberg's results for classical elasticity.

The requirement of vanishing ϵ in the case of infinite bodies (e.g. half-space) may be regarded as equivalent to keeping the area of the load region fixed while the distances of the material points tend to infinity. For beams where we apply loads at the ends, ϵ is actually H/L, where H is the beam's height and $2L$ is the beam's length.

If both the surface tractions and double stresses are confined to several distinct portions of its surface, each lying within a part of the surface of radius ϵ, then the displacements are of a smaller order of magnitude in ϵ when both the surface tractions and double stresses are self equilibrated than when they are not.

Thus, we can only state the relative orders of magnitude and not the extend of the region which is influenced. Rigorous comparisons would require the knowledge of the details of the load intensities rather than the load resultants. In the following, we will present examples that will quantify the previous theoretical results.

5. Energy decay along a slender beam

5.1. Energy decay inequality

In this section we approach the Saint-Venant principle using an energy decay inequality in the spirit of Toupin (1965). We use Type I strain-gradient formulation, according to Mindlin (1964). The potential energy density can be stated as

$$W(\epsilon_{pq}, u_{q,rp}) = \frac{1}{2} c_{pqlm}\epsilon_{pq}\epsilon_{lm} + \frac{1}{2} d_{rpqjlm} u_{q,rp} u_{m,jl} = \frac{1}{2}\tau_{pq}\epsilon_{pq} + \frac{1}{2} m_{rpq} u_{q,rp} \tag{40}$$

where $\tau_{pq} = \tau_{qp} = \partial W/\partial \epsilon_{pq}$ is the stress tensor conjugate to ϵ_{ij} and $m_{rpq} = m_{prq} = \partial W/\partial u_{q,rp}$ is the dipolar stress tensor conjugate to $u_{q,rp}$. The internal energy U of a body with volume V and smooth surface S (with unit outward normal vector n_i), in the absence of body forces, is

$$U = \int_V W \,\mathrm{d}V = \frac{1}{2}\int_S [n_p(\tau_{pq} - m_{rpq,r})u_q + n_r m_{rpq} u_{q,p}]\,\mathrm{d}S = \frac{1}{2}\int_S \left(\widetilde{P}_q u_q + \widetilde{R}_q u_{q,p} n_p\right)\mathrm{d}S \tag{41}$$

where $\widetilde{P}_q = n_j(\tau_{jq} - m_{kjq,k}) - [D_j - (D_r n_r)n_j](n_k m_{kjq})$ and $\widetilde{R}_q = n_j n_k m_{jkq}$. Consider a cylinder, as in Fig. 1, with rounded edges, loaded by $\mathbf{P}$ and $\mathbf{R}$ only on A_0 and in such a way that

$$\int_{A_0} \widetilde{P}_q \,\mathrm{d}S = 0 \quad \text{and} \quad \int_{A_0} \widetilde{R}_q \,\mathrm{d}S = 0 \tag{42a}$$

and

$$\widetilde{P}_q = 0 \quad \text{and} \quad \widetilde{R}_q = 0 \tag{42b}$$

on the rest of the surface of the cylinder. To avoid the complications from the jump relations, we assume rounded edges ($E_q = 0$).

Let A_s be the intersection of the cylinder with a plane perpendicular to the generators of the cylinder at a distance s from A_0 and V_s be the volume between section A_s and the right end of the beam. The plane is slightly rounded close to the cylindrical surface. Since the loads are balanced at section A_0, overall equilib-

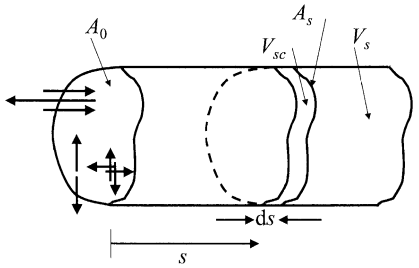

Fig. 1. The cylinder configuration used for the elastic energy decay problem. Self equilibrated loads act at one end ($s = 0$) and the rest of the surface has no load.

rium of V_s requires that the loads are balanced at section A_s as well, i.e. equations similar to (42a) hold on A_s. Following Toupin (1965), we define the modified displacement field $\bar{\mathbf{u}}(\mathbf{x})$

$$\bar{u}_p(\mathbf{x}) = u_p(\mathbf{x}) + a_p + b_{pq}x_q \tag{43}$$

which includes a rigid body translation a_p and a rigid body rotation $2e_{ijk}\,\mathrm{b}jk$, where $b_{ij} = -b_{ji}$. Since rigid body motions do no work on the applied loads and taking into consideration (41)–(42b), we can write the internal energy in V_s as

$$U(s) = \frac{1}{2}\int_{A_s}\left(\widetilde{P}_q\bar{u}_q + \widetilde{R}_q\bar{u}_{q,p}n_p\right)\mathrm{d}A \tag{44}$$

At this point we make use of the Schwartz and Geometric-Arithmetic mean inequalities to assert that (Toupin, 1965, Appendix A)

$$\int_V u_i w_i\,\mathrm{d}V \leqslant \frac{1}{2}\left(\alpha\int_V u_i u_i\,\mathrm{d}V + \frac{1}{\alpha}\int_V w_i w_i\,\mathrm{d}V\right) \tag{45a}$$

for all $\alpha > 0$ and all vector fields $\mathbf{u}(\mathbf{x})$ and $\mathbf{w}(\mathbf{x})$. Using this inequality in Eq. (44), we find

$$U(s) \leqslant \frac{1}{4}\left[\alpha\int_{A_s}\widetilde{P}_m\widetilde{P}_m\,\mathrm{d}S + \frac{1}{\alpha}\int_{A_s}\bar{u}_m\bar{u}_m\,\mathrm{d}S + \sum_{n=1}^{3}\left(\beta_n\int_{A_s}\widetilde{R}_n\widetilde{R}_n\,\mathrm{d}S + \frac{1}{\beta_n}\int_{A_s}\bar{u}_{n,q}\bar{u}_{n,q}\,\mathrm{d}S\right)\right] \tag{45b}$$

for all positive constants α, β_1, β_2, β_3. It should be noted that given any two vectors, say $\widetilde{P}_m$ and $n_j\tau_{jm}$, we can always find a positive constant γ such that the magnitude of $\gamma n_j\tau_{jm}$ is larger than that of $\widetilde{P}_m$, i.e.,

$$\widetilde{P}_m\widetilde{P}_m \leqslant \gamma n_j\tau_{jm}n_k\tau_{km}$$

Also, using the methodology of Toupin (1965, Appendix B), we can show that there exist two positive constants c_M and d_M (e.g. the maximum positive eigenvalues of c_{pqlm} and d_{rpqjlm}, respectively, if grouped as matrices) such that

$$\widetilde{P}_n\widetilde{P}_n \leqslant \gamma n_j\tau_{jm}n_k\tau_{km} \leqslant 2\gamma c_M W \tag{45c}$$

and (see also Berglund, 1977, p. 320)

$$\widetilde{R}_n\widetilde{R}_n = n_j n_k m_{jkn}\; n_p n_q m_{pqn} \leqslant n_j m_{jkn}\; n_p m_{pkn} \leqslant 2d_M W \tag{45d}$$

Using (45c) and (45d) in (45b), we conclude that

$$U(s) \leqslant \frac{1}{4}\left\{2[\alpha\gamma c_M + (\beta_1+\beta_2+\beta_3)d_M]\int_{A_s}W\,\mathrm{d}S + \frac{1}{\alpha}\int_{A_s}\bar{u}_m\bar{u}_m\,\mathrm{d}S + \sum_{n=1}^{3}\frac{1}{\beta_n}\int_{A_s}\bar{u}_{n,q}\bar{u}_{n,q}\,\mathrm{d}S\right\} \tag{46}$$

Integrating the above inequalities in the volume V_{sc} of the beam region between the two sections at s and $s + \mathrm{d}s$, we obtain

$$\int_s^{s+\mathrm{d}s}U(s^*)\,\mathrm{d}s^* \leqslant \frac{1}{4}\left\{2[\alpha\gamma c_M + (\beta_1+\beta_2+\beta_3)d_M]\int_{V_{sc}}W\,\mathrm{d}V + \frac{1}{\alpha}\int_{V_{sc}}\bar{u}_m\bar{u}_m\,\mathrm{d}V + \sum_{n=1}^{3}\frac{1}{\beta_n}\int_{V_{sc}}\bar{u}_{n,q}\bar{u}_{n,q}\,\mathrm{d}V\right\} \tag{47}$$

Assuming that the displacements and their derivatives are bounded in the beam, we can select the constants β_n so that

$$\beta_1 = \alpha\frac{\int_{V_{sc}}\bar{u}_{n,1}\bar{u}_{n,1}\,\mathrm{d}V}{\int_{V_{sc}}\bar{u}_m\bar{u}_m\,\mathrm{d}V}, \quad \beta_2 = \alpha\frac{\int_{V_{sc}}\bar{u}_{n,2}\bar{u}_{n,2}\,\mathrm{d}V}{\int_{V_{sc}}\bar{u}_m\bar{u}_m\,\mathrm{d}V}, \quad \beta_3 = \alpha\frac{\int_{V_{sc}}\bar{u}_{n,3}\bar{u}_{n,3}\,\mathrm{d}V}{\int_{V_{sc}}\bar{u}_m\bar{u}_m\,\mathrm{d}V} \tag{48}$$

Next, we use the methodology of Toupin (1965) to obtain an upper bound for $\int_{V_{sc}} \bar{u}_m \bar{u}_m \, dV$. It follows from Rayleigh's principle that, for a proper choice of the rigidbody-displacement constants a_i and b_{ij},

$$\int_{V_{sc}} \bar{u}_m \bar{u}_m \, dV \leqslant \frac{1}{\rho \omega_0^2} \int_{V_{sc}} W \, dV \tag{49}$$

where ρ is the mass density of the elastic body and ω_0 the lowest characteristic frequency of free vibration of the part of the body included in V_{sc}. We note that ω_0 can be found from the solution of the eigenvalue problem

$$\left(\tau_{pq}^{(k)} - m_{rpq,r}^{(k)}\right)_{,p} + \rho \omega_k^2 u_q^{(k)} = 0 \quad \text{(no sum over } k\text{)} \tag{50}$$

with zero loads on the boundary of V_{sc}. In Eq. (50), $u_q^{(k)}$ is the kth eigenfunction. The stresses $\tau_{pq}^{(k)}$ and $m_{rpq}^{(k)}$ can be obtained from the displacements $u_q^{(k)}$ through the constitutive equations.

The inequality (47), together with (48) and (49) can be stated as

$$\int_s^{s+ds} U(s^*) \, ds^* \leqslant \frac{1}{2} \left[\alpha \gamma c_M + (\beta_1 + \beta_2 + \beta_3) d_M + \frac{2}{\alpha \rho \omega_0^2} \right] \int_{V_{sc}} W \, dV \tag{51}$$

Following Berglund (1977), we define

$$\sigma = \max \left[\gamma c_M, d_M \frac{(\beta_1 + \beta_2 + \beta_3)}{\alpha} \right] \tag{52}$$

and

$$h(\alpha, \sigma) = \alpha \sigma + \frac{1}{\alpha \rho \omega_0^2} \tag{53}$$

Then, Eq. (51) implies

$$\int_s^{s+ds} U(s^*) \, ds^* \leqslant h \int_{V_{sc}} W \, dV = h[U(s) - U(s + ds)] \tag{54a}$$

Since $U(s)$ is a positive and non-increasing function of s, we have that

$$U(s + ds) \, ds \leqslant \int_s^{s+ds} U(s^*) \, ds^* \tag{54b}$$

Therefore, using (54a), we conclude that

$$U(s + ds) \, ds \leqslant h[U(s) - U(s + ds)] \tag{54c}$$

In the limit $ds \to 0$, the last inequality implies that

$$U \leqslant -h \frac{dU}{ds} \tag{54d}$$

Integrating the last inequality from 0 to s, we conclude that

$$U(s) \leqslant U(0) \exp\left[-\frac{s}{h}\right] \tag{54e}$$

The minimum value of h with respect to α is

$$\min h = 2\sqrt{\frac{\sigma}{\rho \omega_0^2}} \quad \text{when } \alpha = \sqrt{\frac{1}{\sigma \rho \omega_0^2}} \tag{55}$$

Inequality (54e) provides an upper bound for the elastic strain energy

$$U(s) \leqslant U(0) \exp\left[-\frac{s}{\min h}\right] \tag{56}$$

In the above expression, $U(0)$ is the internal energy of the whole beam and $U(s)$ is the portion of the energy stored in the part of the beam between the right, load-free, end-section and the cross section at a distance s from the loaded left end. Inequality (56) is similar to the well-known exponential decay of the elastic energy found in classic elasticity (Toupin, 1965) and in micropolar media (Berglund, 1977). Note that $\rho\omega_0^2$ can be considered as the square of the characteristic frequency of a section of the cylinder with unit mass density. Therefore, the rate of the exponential decay of the elastic energy is determined by the material constants and the geometry of the beam.

5.2. Example: Slender beam

Fig. 2 shows a plane strain beam of length L. The thickness of the beam is $H(H < L)$ and the coordinates (x_1, x_2) are at the loaded end of the beam (self-equilibrated), so that $L \leqslant x_1 \leqslant 0$ and $-H/2 \leqslant x_2 \leqslant H/2$. We will use the simplest constitutive Eqs. (A.1), (A.2), (A.5), given in Appendix A. For a slice of a beam at a distance $x_1 = s$, we assume $u_2 \approx u_2(x_2)$ and the eigenvalue problem (50) becomes

$$\frac{\partial^2 u_2^{(k)}}{\partial x_2^2} - l^2 \frac{\partial^4 u_2^{(k)}}{\partial x_2^4} + \frac{\rho\omega_k^2}{E} = 0 \tag{57}$$

where E is the elastic modulus and l is the microstructural length of the beam. The only boundary condition that is not satisfied trivially is

$$\widetilde{P}_2^{(k)} = \tau_{22}^{(k)} - m_{222,2}^{(k)} = E\frac{\partial u_2^{(k)}}{\partial x_2} - El^2 \frac{\partial^3 u_2^{(k)}}{\partial x_2^3} = 0 \quad \text{at } x_2 = \pm\frac{H}{2} \tag{58}$$

A long wave eigen-solution of the above, one-dimensional, free vibration problem is

$$u_2^{(0)} = \sin\frac{\pi x_2}{H} \text{ and } \frac{\rho\omega_0^2}{E} = \left(\frac{\pi}{H}\right)^2 \left[1 + \left(\frac{\pi l}{H}\right)^2\right] \tag{59a}$$

In this case $c_M \approx E$ and $d_M \approx El^2$. Using the choice (59a), we compute $\beta_2^{(0)}/\alpha = (\pi/H)^2$. The corresponding $\tau_{22}^{(0)}$ and $\widetilde{P}_2^{(0)}$ are

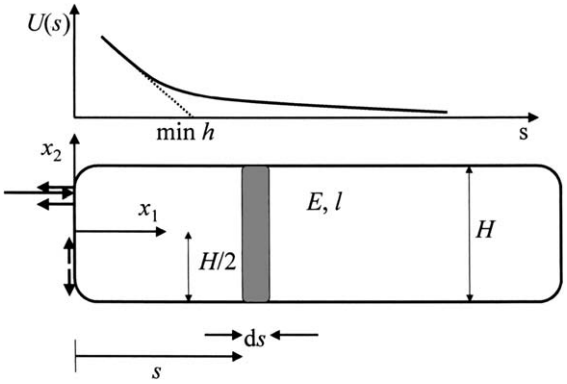

Fig. 2. The plane strain beam used for the arguments of the elastic energy exponential decay.

$$\tau_{22}^{(0)} = E\frac{\partial u_2^{(k)}}{\partial x_2} = \frac{\pi E}{H}\cos\frac{\pi x_2}{H} \tag{59b}$$

and

$$\widetilde{P}_2^{(0)} = E\frac{\partial u_2^{(k)}}{\partial x_2} - El^2\frac{\partial^3 u_2^{(k)}}{\partial x_2^3} = \left[1+\left(\frac{\pi l}{H}\right)^2\right]\tau_{22}^{(0)} \tag{59c}$$

In most practical cases $0 \leqslant l/H \leqslant 1/\pi = 0.318$; therefore $\widetilde{P}_2^{(0)} \leqslant 2\tau_{22}^{(0)}$, and

$$\widetilde{P}_2^{(0)}\widetilde{P}_2^{(0)} \leqslant 4\tau_{22}^{(0)}\tau_{22}^{(0)} \tag{59d}$$

i.e., $\gamma^{(0)} = 4$ in this case.

If we accept the $\beta_2^{(0)}$ and $\gamma^{(0)}$ values as representative, then the corresponding estimates for σ and h are

$$\sigma = \max\left[4E, \left(\frac{\pi l}{H}\right)^2 E\right] = 4E \quad \text{and} \quad \min h = \frac{4}{\pi}\frac{H}{\sqrt{1+(\pi l/H)^2}} \tag{60}$$

The exponential decay rate of the elastic energy is increasing with the microstructural length l

$$U(s) \leqslant U_0 \exp\left[-\frac{\pi}{4}\frac{s}{H}\sqrt{1+\left(\frac{\pi l}{H}\right)^2}\right] \tag{61}$$

6. Numerical examples and comparisons with analytical results

Quantitative evaluation of the Saint-Venant principle would require full solutions of key problems such as bending, axial loading and shearing of beams. Classic elasticity has dealt with such problems using theoretical solutions, e.g. Filon (1903). In the case of strain-gradient elasticity, beam solutions already exist for particular cases of constitutive equations and loading, Koiter (1964), Papargyri-Beskou et al. (2003) and Tsepoura et al. (2002).

In the present work, we solved two-dimensional plane strain problems using the finite element method. We examined in particular the simplest isotropic strain-gradient model with explicit constitutive forms given in Appendix A (Eqs. (A.1), (A.2), (A.5)). Although simple, the fore-mentioned constitutive model is less satisfactory in complex cases such as crack-tip fields.

A novel finite element was used that was developed by Amanatidou and Aravas (2002) together with the ABAQUS (2003) general purpose finite element code. It is a plane-strain, nine-node, mixed element with

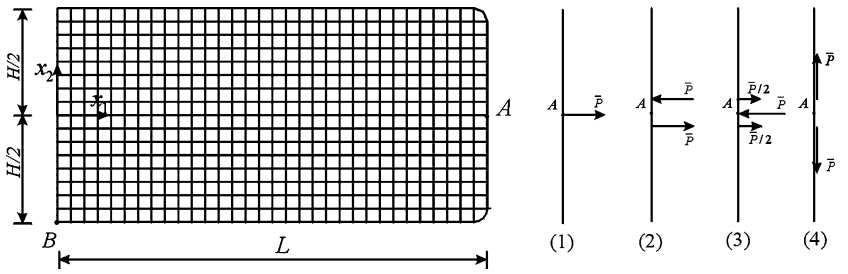

Fig. 3. Half of a rectangular block of material with length $2L$ and height H, with rounded corners. The coordinate system (x_1, x_2) is indicated (plain strain). The four loading cases applied at the vicinity of point A are shown. Also shown is the 32×16, 9-noded finite element mesh used in the calculations of the vertical displacement at point B. ($L = 0.008$ m, $H = 0.04$ m, $e = 0.25\times 10^{-2}$ m, $\overline{P} = 1$ GN/m, $E = 85$ GPa, $\nu = 0.26, l = 0.16\times 10^{-2}$ m).

independent isoparametric interpolation for the displacements u_i, their tangent derivatives $u_{i,j} - u_{i,k}n_k n_j$ and their third derivatives $u_{k,iji}$. The element has two displacements and four tangent derivatives, as degrees of freedom at each of the nine nodes of the element. In addition the element has one third order derivative as degree of freedom at each of the four corner nodes of the element. Therefore, each element has a total of 70 degrees of freedom with bi-quadratic Lagrangian interpolation for u_i and $u_{i,j} - u_{i,k}n_k n_j$ and bilinear interpolation for $u_{k,iji}$. A patch of at least 2×2 elements was found to have none zero eigenvalue.

We considered a rectangular block of material with length $2L$, height H, and rounded corners ($E_i = 0$). Fig. 3 shows one half of the block. Loads were applied near point A ($x_1 = L, x_2 = 0$) and its symmetric point ($x_1 = -L, x_2 = 0$) with respect to the x_2 axis. Along the symmetry line $x_1 = 0$, $u_1 = 0$ and $u_{2,1} = 0$. At the origin ($x_1 = 0, x_2 = 0$)$u_2 = 0$, to eliminate any rigid body motion in the x_2 direction. The four loading cases are shown in Fig. 3. The first case corresponds to a non-zero resultant force; in the second case the resultant force vanishes; in the third and fourth cases the forces are in astatic equilibrium. The radius of roundness and the distance that defines the location of the applied loads near point A were equal to one element side e. The 32×16 finite element mesh ($e = H/16$) with the type of elements mentioned above is also shown in Fig. 3. The calculations were carried out for $L/H = 2$, $l/H = 0.04$ (l is the microstructural length), Young's modulus $E = 85$ GPa and Poisson ratio $\nu = 0.26$. These properties relate to those of marble, Vardoulakis et al. (1998).

We define the dimensionless quantity $v^{B(i)} = u_2(B)E/\overline{P}$, where $u_2(B)$ is the x_2 displacement of point B $(x_1 = -H/2,\ x_2 = 0)$, $\overline{P}$ is the total applied load per unit of out-of-plane thickness. The calculated values of $v^{B(i)}$ for the four types of loading ($i = 1, 2, 3, 4$, as in Fig. 3) are

$$v^{B(1)} = 1.63 \times 10^{-1}, \quad v^{B(2)} = 6.03 \times 10^{-2}, \quad v^{B(3)} = 1.84 \times 10^{-4}, \quad v^{B(4)} = -1.05 \times 10^{-4}$$

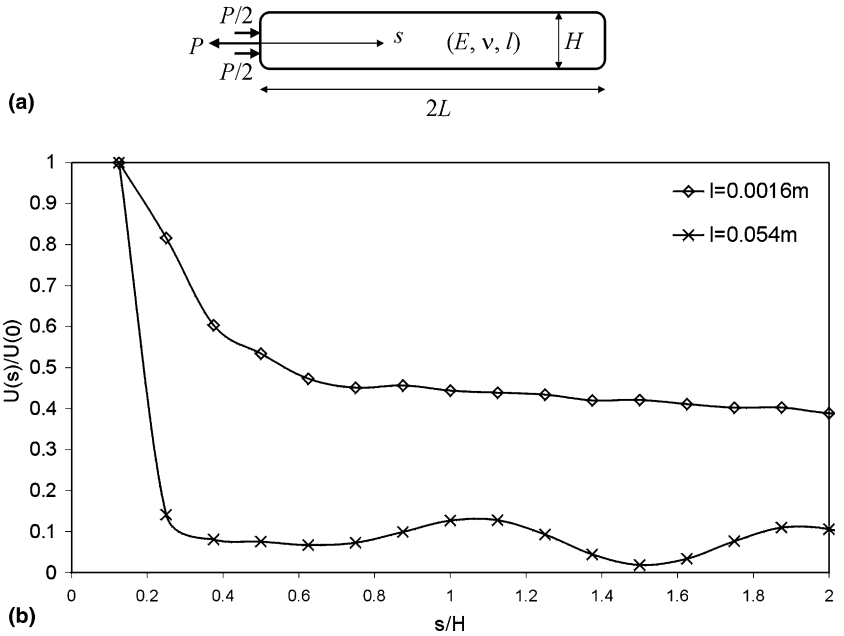

Fig. 4. (a) Configuration used for elastic energy decay problem (plane-strain, $2L = H = 10$). At one end acts a self equilibrated load (indicated by load case (3) in Fig. 3) and the other end is free. A uniform mesh of 8×80, 9-noded elements was used (element size 1/8 m) with microstructural lengths $l/H = 0.0016$ and $l/H = 0.054$. (b) Normalized energy $U(s)/U(0)$ versus normalized axial distance s/H.

If we identify $\epsilon = e/H = 0.0625$, then it is clear that the following inequalities hold:

$$\mathrm{O}(v^{B(2)}) \leqslant \mathrm{O}(\epsilon v^{B(1)}), \quad \mathrm{O}(v^{B(3)}) \leqslant \mathrm{O}(\epsilon^2 v^{B(1)}) \quad \mathrm{O}(v^{B(4)}) \leqslant \mathrm{O}(\epsilon^2 v^{B(1)})$$

thus verifying the aforementioned "Saint-Venant principle". For $L/H = 4$, the results for $v^{B(1)}$ and $v^{B(2)}$ remain almost the same, whereas $v^{B(3)} = -7.68 \times 10^{-9}$, which means that away from the loaded-end there is practically no deformation. This is expected since loading case (3) gives no force and no moment resultant on the surface. For completeness we state the corresponding results for the classic elastic case ($l = 0$).

$$v^{B(1)} = 1.64 \times 10^{-1}, \quad v^{B(2)} = 6.15 \times 10^{-2}, \quad v^{B(3)} = 1.96 \times 10^{-4}, \quad v^{B(4)} = -1.44 \times 10^{-4}$$

The results confirm that the strain gradient elasticity predicts stiffer response than the classic elasticity.

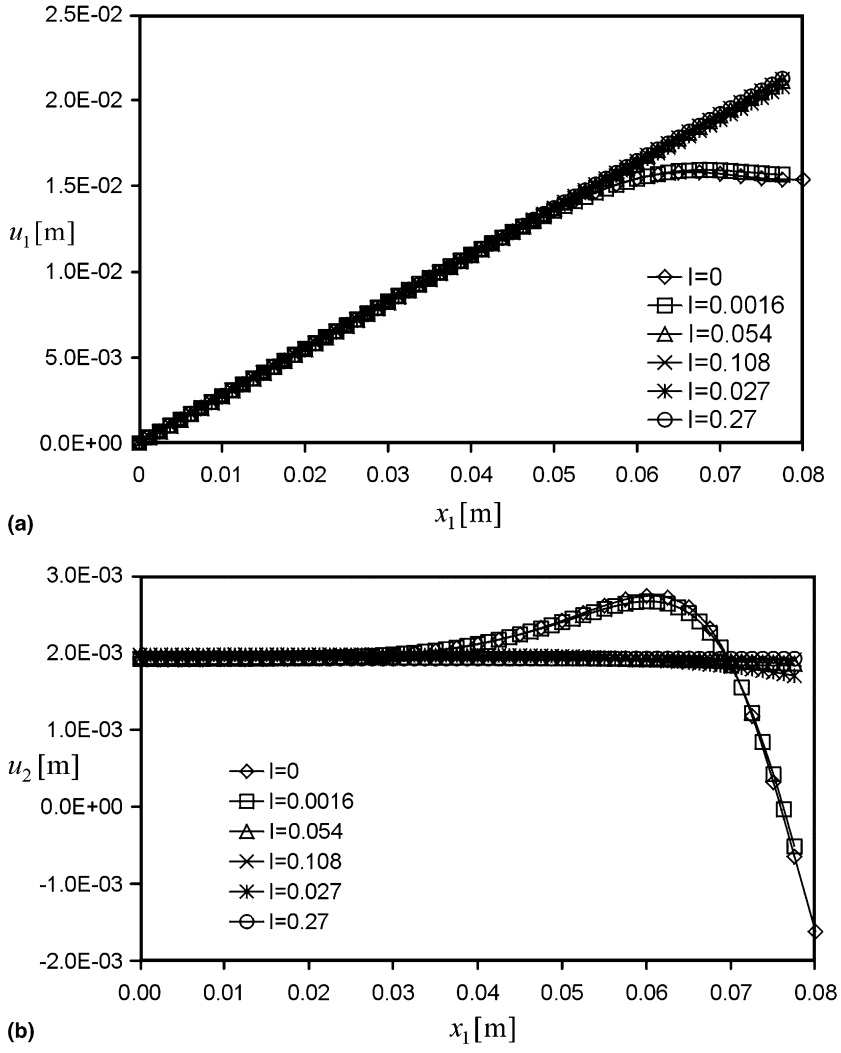

Fig. 5. (a) The displacement u_1 along the side $x_2 = -H/2$ for loading case 1 of Fig. 3 (uniaxial tension, $l = 0$,0.027, 0.054,0.108 m, beam prediction max $u_1 = 0.022$ m). (b) The displacement u_2 along the side $x_2 = -H/2$ for loading case 1 of Fig. 3 (uniaxial tension, $l = 0$, 0.027, 0.054, 0.108 m, beam prediction $u_2 = -0.0019$ m).

To investigate the energy decay along a slender beam, we analyzed a beam with $2L/H = 10$ under self equilibrated forces, as shown in Fig. 4a. A uniform mesh of 8×80 elements was used (element size 1/8 m) with microstructural lengths $l/H = 0.0016$ and $l/H = 0.054$. The normalized numerical results of $U(s)/U(0)$ versus s/H are plotted in Fig. 4b. The numerical results are in accord with our theoretical finding that the energy decays faster with increasing microstructural length.

6.1. The plane-strain uniaxial tension problem

To investigate the influence of the size of the microstructural length l, we examined the uniaxial tension (described in Fig. 3 as case 1) for $2L = 0.16$ m and $l = 0,0.027, 0.054, 0.108$ m. Fig. 5a shows the u_1 displacements along the side $x_2 = -H/2$ and Fig. 5b shows the u_2 displacements along the same side. Tsepoura et al. (2002) have solved the uniaxial tension problem and adjusting their analytical results we obtain

$$u_1(x_1) = \frac{\overline{P}(1-\nu^2)}{HE} x_1, \quad u_2(x_1) = -\frac{\nu}{(1-\nu)} \frac{\overline{P}(1-\nu^2)}{HE} \frac{H}{2} \tag{62}$$

It is clear that the end effect erodes the above approximation. We note that increasing the microstructural length, the region of validity of the homogeneous solution increases, in accord with the theoretical prediction.

6.2. The plain strain three-point bending problem

Next, we solved the two-dimensional three-point bending problem (plain strain, out-of-plane dimension 1m). The configuration and loading are indicated in Fig. 6. Due to symmetry, we modelled one half of the beam. The mesh layout is shown in Fig. 3.

The finite element results for $\overline{P} = 49$ kN/m, $H = 0.1$ m and $2L = 0.4$ m are shown in Fig. 7. The vertical deformation $u_2(x_1)$ of the middle-line is shown in Fig. 7a. Plots of the axial strain distribution $\epsilon_{11}(x_2)$ at locations $x_1/L = 0, 0.2, 0.2, 0.3$ for the classic case $l = 0$ m are shown in Fig. 7b. Plots of the axial strain distribution $\epsilon_{11}(x_2)$ at locations $x_1/L = 0,\ 0.1, 0.2, 0.3$ for a microstructural length $l = 0.054$ m are shown in Fig. 7c. Similar results for $\overline{P} = 792.5$ kN/m, $H = 0.04$ m and $2L = 0.16$ m are shown in Fig. 8. It is clear that the strain gradient analysis predicts a stiffer response, as expected. Using the bending theory of Papargyri-Beskou et al. (2003), Giannakopoulos and Stamoulis (in preparation) predict the deflection of the midsection of the beam to be

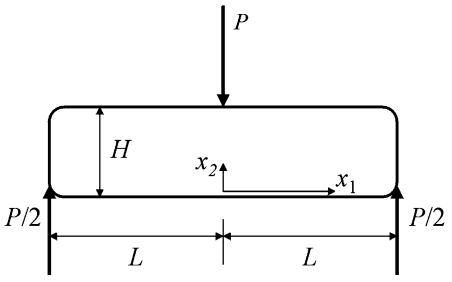

Fig. 6. Configuration used for the three-point bending analysis (plane-strain, $2L/H = 4$). Material constants: $E = 85$ GPa, $\nu = 0.26$ and $l = 0.054$ or $l = 0$ m. The finite element mesh is shown in Fig. 3. (a) $\overline{P} = 31.7$ kN/m with $2L = 0.4$ m, (b) $\overline{P} = 4.9$ kN/m with $2L = 0.16$ m.

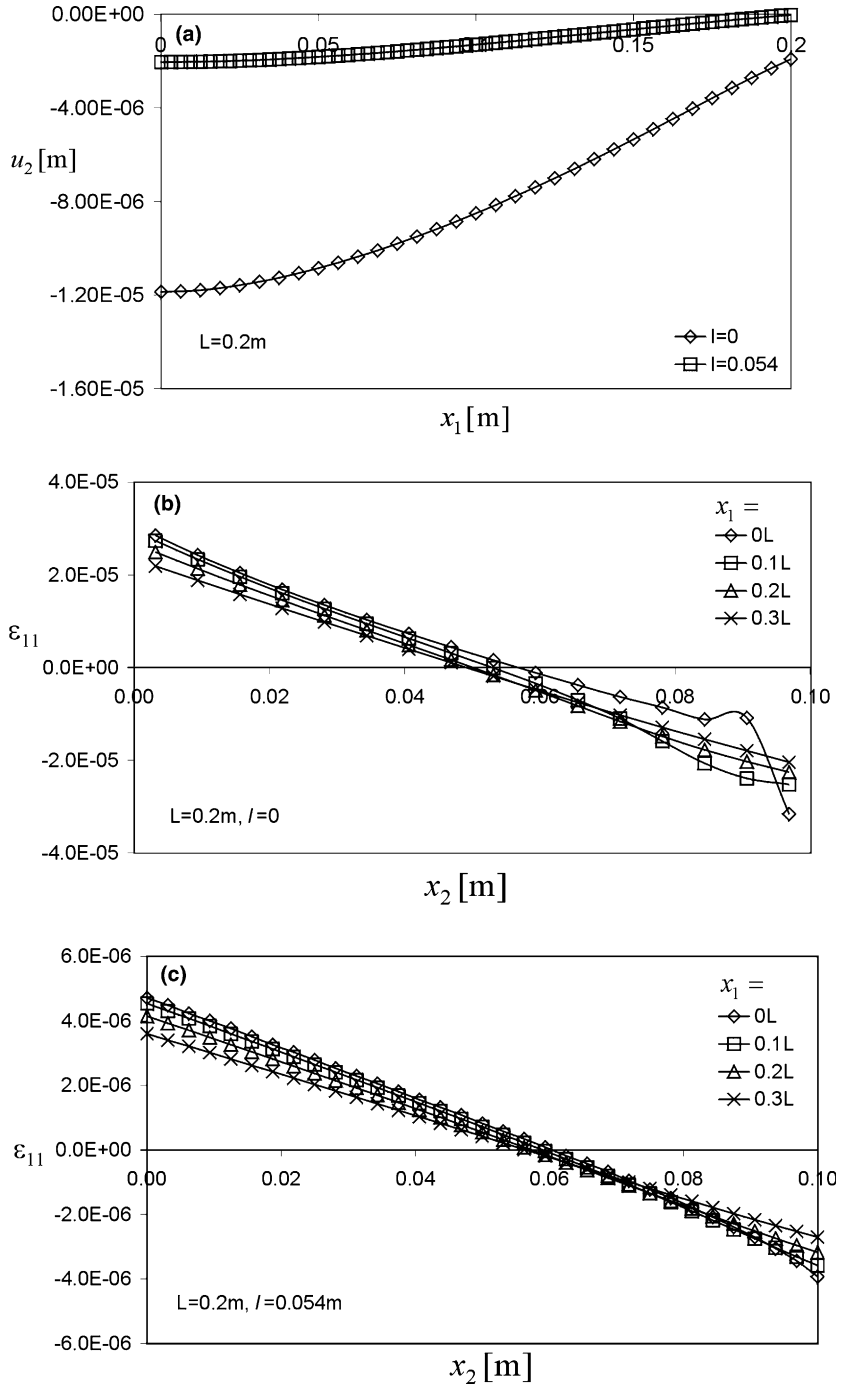

Fig. 7. The finite element results for the three-point bending described in Fig. 6 with $\overline{P} = 49$ kN/m, $H = 0.1$ m and $2L = 0.4$ m. (a) Vertical deformation $u(x_1)$ of the middleline $x_2 = H/2$. (b) Axial strain distribution $\epsilon_{11}(x_2)$ at locations $x_1/L = 0, 0.2, 0.2, 0.3$ (case $l = 0$ m). (c) Axial strain distribution $\epsilon_{11}(x_2)$ at locations $x_1/L = 0, 0.2, 0.2, 0.3$ (case $l = 0.054$ m).

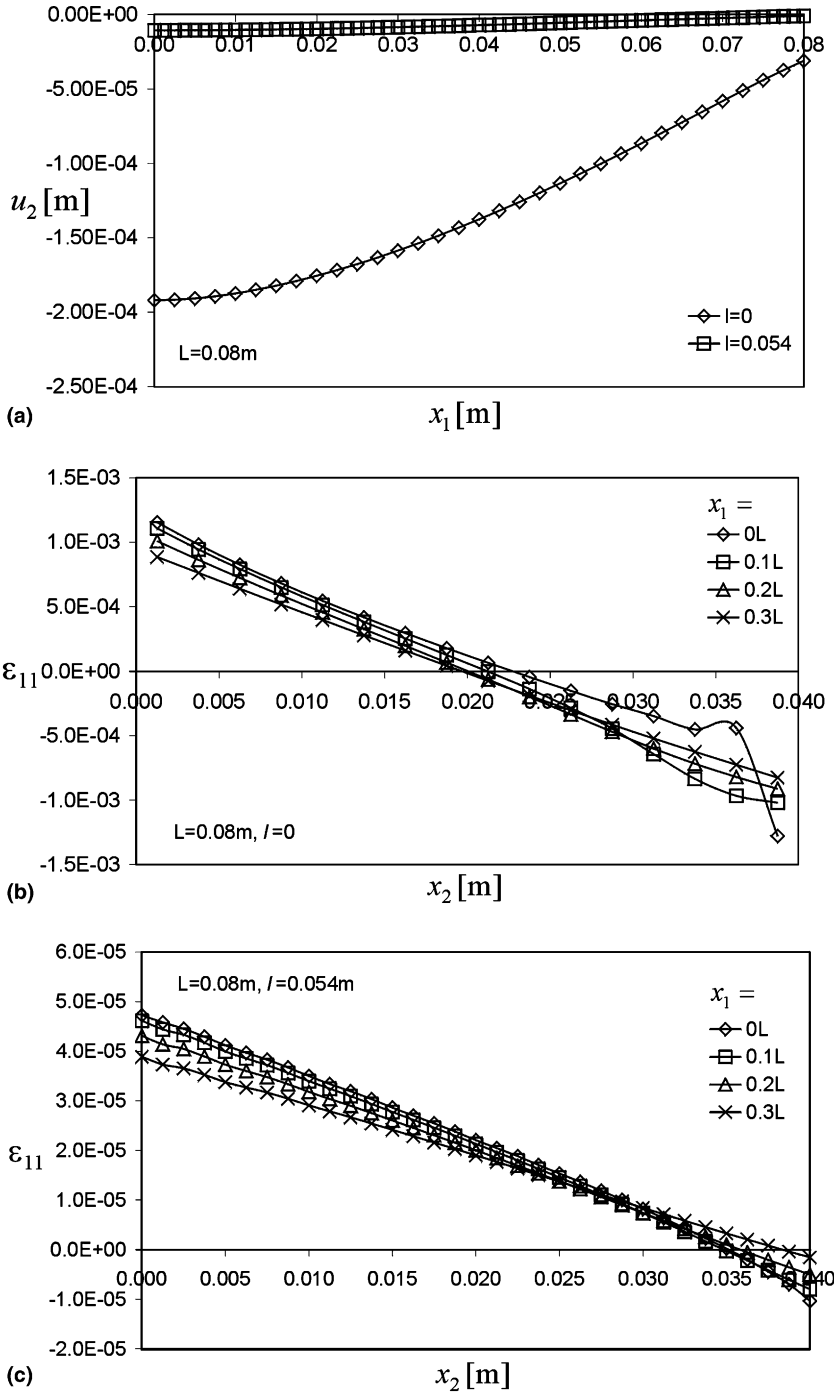

Fig. 8. The finite element results for the three-point bending described in Fig. 6 with $\overline{P} = 792.5$ kN/m, $H = 0.04$ m and $2L = 0.16$ m. (a) Vertical deformation $u(x_1)$ of the middle-line $x_2 = H/2$. (b) Axial strain distribution $\epsilon_{11}(x_2)$ at locations $x_1/L = 0, 0.2, 0.2, 0.3$ (case $l = 0$ m). (c) Axial strain distribution $\epsilon_{11}(x_2)$ at locations $x_1/L = 0, 0.2, 0.2, 0.3$ (case $l = 0.054$ m).

$$u_2(x_1=0)=-\frac{6\overline{P}L^3}{EH^3}\left\{\frac{1}{3}-\left(\frac{l}{L}\right)^2\left(\cosh\left(\frac{L}{l}\right)+\frac{1}{\cosh\left(\frac{L}{l}\right)}+\frac{L}{l}\tanh\left(\frac{L}{l}\right)-1\right)\right.$$
$$\left.+\left(\frac{l}{L}\right)^3\left(\tanh\left(\frac{L}{l}\right)+\frac{L}{l}\tanh\left(\frac{L}{l}\right)\sinh\left(\frac{L}{l}\right)\right)\right\} \tag{63}$$

Note that Eq. (63) predicts the classic result in the limit $l\to 0$

$$u_2(x_1=0)=-\frac{2\overline{P}L^3}{EH^3}(l\to 0) \tag{64}$$

The end deflection is decreasing monotonically with l/L, predicting a stiffer response. Using (64), we predict $u_2(0)=-0.92\times10^{-5}$ m for $\overline{P}=49$ kN/m, $H=0.1$ m and $2L=0.4$ m and $u_2(0)=-1.49\times10^{-4}$ m for $\overline{P}=792.5$ kN/m, $H=0.04$ m and $2L=0.16$ m. These results compare very well with the finite element computations, shown in Figs. 7a and 8a, respectively. For $l=0.054$ m, Eq. (63) predicts that the deflection at the beam's center is 2.2 and 6.4 times smaller than the ones predicted by the classic elasticity, for the cases shown in Figs. 7 and 8, respectively. The finite elements predict factors of 5 and 7 for the corresponding cases. Therefore, the estimate of Eq. (63) is useful for slender beams ($2L/H\gg 4$).

The finite element analysis indicates that the Bernoulli-beam assumption of linear variation of the axial strains ϵ_{11} is reasonable, however, $\epsilon_{11}\neq kx_2$. Therefore, the small "punch effect" (the perturbation of the normal strains by an axial tensile strain at the midspan) predicted by Timoshenko and Goodier (1970) for the classic case ($l=0$), appears to be pronounced and non-local for the gradient case ($l\neq 0$). Classic elasticity predicts a maximum shift of the neutral axis of $0.17H$, localized at the center of the beam. The gradient elasticity predicts a shift of the neutral axis along the whole length of the beam. This newly discovered "punch effect" seems to increase with the ratio l/H and could bring most of the beam into tensile straining. Thus, we can conclude that the Bernoulli-beam assumption requires $2L/H\gg 4$ and $H/l\gg 2$. The first restriction is well known from classic elasticity. The last restriction is novel and is due to the strain gradient model of the beam.

7. Conclusions

Nano- and microelectromechanical devices use extensively structural components in the form of beams, plates, shells and membranes. In such cases, the material microstructural lengths become important and strain gradient elasticity can provide useful material modelling. The range of applications can extend to large scales, whenever materials can be modelled with gradient elasticity, for example fiber composites and concrete. The approximate solutions of problems of extension, torsion and flexure of slender bodies rely on the Saint-Venant principle. The present work investigated the validity of Saint-Venant's principle in the context of the linear strain gradient elasticity. A reciprocity theorem analogous to Betti's theorem was proven first, suggesting constitutive restrictions that preclude surface terms and body double-forces in the formulation. As a side result, the powerful Castigliano's theorems were obtained. It was shown that the order of magnitude of the displacements are in accord with a Sternberg's statement of the Saint-Venant principle. In addition, an exponential decay for the elastic energy was found valid for a prismatic beam with self-equilibrated loaded ends. It was found that the energy decay becomes stronger with increasing microstructural length. The cases of stretching, shearing and bending of a beam were examined in detail, using a novel finite element methodology. The numerical results confirmed the theoretical findings. Regarding the bending of beams, it was found that the usual assumption of the Bernoulli beam theory is invalid for cases where the microstructural length is more than half of the beam's thickness.

Acknowledgements

The work is part of the project of "Fatigue of MEMS" that is ongoing in the Laboratory for Strength of Materials and Micromechanics of the Department of Civil Engineering, University of Thessaly. We would like to thank Prof. H. Georgiadis of the National Technical University of Athens for bringing to our attention the unpublished reciprocity form and Castigliano's theorems that his group found for the isotropic case, in full accord with our general results.

Appendix A. Isotropic material response

According to Mindlin (1964), the most general form of a Type II, isotropic constitutive law is

$$\tau_{ij} = \lambda\delta_{ij}\epsilon_{kk} + 2\mu\epsilon_{ij} \tag{A.1}$$

$$\mu_{pqr} = \frac{1}{2}a_1(\delta_{pq}\kappa_{rii} + 2\delta_{qr}\kappa_{iip} + \delta_{rp}\kappa_{qii}) + 2a_2\delta_{qr}\kappa_{pii} + a_3(\delta_{pq}\kappa_{iir} + \delta_{pr}\kappa_{iiq}) + 2a_4\kappa_{pqr} + a_5(\kappa_{rpq} + \kappa_{qrp}) \tag{A.2}$$

where $\kappa_{ijk} = \epsilon_{jk,i}$, δ_{ij} is Kronecker's delta, $(a_1, a_2, a_3, a_4, a_5)$ are material constants and λ, μ are the familiar Lame's constants that are connected with the elastic modulus E and the Poisson's ration v by

$$\mu = \frac{E}{2(1+v)}, \quad \lambda = \frac{vE}{(1+v)(1-2v)}$$

Necessary and sufficient conditions for positive definiteness of the potential energy density, leading to unique solutions, are

$$\begin{aligned} &\mu > 0, \quad 3\lambda + 2\mu > 0 \\ &\bar{d}_1 > 0, \quad -\bar{d}_1 < \bar{d}_2 < \bar{d}_1 \\ &\bar{a}_2 > 0, \quad 3\bar{a}_1 + 2\bar{a}_2 > 0, \quad \bar{f} > 0 \end{aligned} \tag{A.3}$$

where

$$\begin{aligned} 18\bar{d}_1 &= -2a_1 + 4a_2 + a_3 + 6a_4 - 3a_5 \\ 18\bar{d}_2 &= 2a_1 - 4a_2 - a_3 \\ 3\bar{a}_1 &= 2(a_1 + a_2 + a_3) \\ \bar{a}_2 &= a_2 + a_5 \\ 3\bar{f} &= a_1 + 4a_2 - 2a_3 \end{aligned} \tag{A.4}$$

A simpler isotropic constitutive model which is used extensively (e.g. Ru and Aifantis (1993) and Georgiadis et al. (2004)), when expressed in Mindlin's framework, results in

$$a_1 = a_3 = a_5 = 0, \quad a_4 = l^2\mu, \quad a_2 = l^2\lambda/2 \tag{A.5}$$

where l is a microstructural length ($\mu > 0, \lambda > 0$).

Another simple isotropic case can be formulated to model the couple-stress constitutive equations of Koiter (1964), resulting in

$$a_1 = 4\eta\mu l^2, \quad a_2 = a_3 = -a_1, \quad a_4 = 2\mu l^2(1+\eta) = -a_5 \tag{A.6}$$

where η is a dimensionless constant ($-1 < \eta < 1$).

References

ABAQUS, 2003. Version 6.4 Finite Element Code, ABAQUS, Inc. Hibbitt, Karlsson and Sorensen, Inc, Pawtucket, RI.

Amanatidou, E., Aravas, N., 2002. Mixed finite element formulations of straingradient elasticity problems. Comp. Meth. Appl. Mech. Engng. 191, 1723–1751.

Berglund, K., 1977. Generalization of Saint Venant's principle to micropolar continua. Arch. Ratl. Mech. Anal. 64, 317–326.

Boley, B.A., 1958. Some observations on Saint-Venant's principle. In: Proceedings of the 3rd US National Congress of Applied Mechanics, Providence, R.I., pp. 259–264.

Filon, L.N.G., 1903. On an approximate solution for the bending of a beam of rectangular cross section under any system of load, with special reference to points of concentration or discontinuous loading. Philos. Trans. Ser. A 201, 63–155.

Georgiadis, H., Vardoulakis, I., Velgaki, E.G., 2004. Dispersive Rayleigh-wave propagation in microstructured solids characterized by dipolar gradient elasticity. J. Elasticity 74, 17–45.

Giannakopoulos, A.E., Stamoulis, K., in preparation. Structural analysis of MEMS.

Horgan, C.O., Knowles, J.K., 1983. Recent developments concerning Saint-Venant's principle. Adv. Appl. Mech. 23, 179–269.

Koiter, W.T., 1964. Couple stresses in the theory of elasticity, I and II. Proc. K. Ned. Akad. Wet. B 67, 17–44.

Love, A.E.H., 1927. A Treatise on the Mathematical Theory of Elasticity, fourth ed. Dover Publication.

Mindlin, R.D., 1964. Micro-structure in linear elasticity. Arch. Ratl. Mech. Anal. 16, 51–78.

Naghdi, P.M., 1960. On Saint-Venant's principle: elastic shells and plates. J. Appl. Mech. 82, 417–422.

Nakamura, S., Lakes, R.S., 1995. Finite element analysis of Saint-Venant end effects in micropolar elastic solids. Eng. Comput. 12, 571–587.

Papargyri-Beskou, S., Tsepoura, K.G., Polyzos, D., Beskos, D.E., 2003. Bending and stability analysis of gradient elastic beams. Int. J. Solids Struct. 40, 385–400.

Polyzos, D., Tsepoura, K.G., Tsinopoulos, S.V., Beskos, D.E., 2003. A boundary element method for solving 2-D and 3-D static gradient elastic problems. Part I: Integral formulation. Comp. Meth. Appl. Mech. Engng. 192, 2845–2873.

Ru, C.Q., Aifantis, E.C., 1993. A simple approach to solve boundary-value problems in gradient elasticity. Acta Mech. 101, 59–68.

Sternberg, E., 1954. On Saint-Venant's principle. Quart. Appl. Math. 11, 393–402.

Timoshenko, S.P., Goodier, J.N., 1970. Theory of Elasticity. McGraw-Hill, New York.

Toupin, R.A., 1965. Saint-Venant's principle. Arch. Ratl. Mech. Anal. 18, 83–96.

Tsepoura, K.G., Papargyri-Beskou, S., Polyzos, D., Beskos, D.E., 2002. Static and dynamic analysis of a gradient-elastic bar in tension. Arch. Appl. Mech. 72, 483–497.

Vardoulakis, I., Exadactylos, G., Kourkoulis, S.K., 1998. Bending of marble with intrinsic length scales: a gradient theory with surface energy and size effects. J. Phys. IV France 8, 399–406.